

## Sub-leading flow modes in PbPb collisions at $\sqrt{s_{NN}} = 2.76$ TeV from HYDJET++ model

Jovan Milosevic<sup>1,3,a</sup>, Predrag Cirkovic<sup>2</sup>, Damir Devetak<sup>1</sup>, Milos Dordevic<sup>1</sup>, and Milan Stojanovic<sup>1</sup>

<sup>1</sup>University of Belgrade and Vinca Institute of Nuclear Sciences, P.O. Box 522, 11001 Belgrade, Serbia

<sup>2</sup>University of Belgrade and Institute of physics, P.O. Box 68, 11081 Belgrade, Serbia

<sup>3</sup>University of Oslo, Department of Physics, Oslo, Norway

**Abstract.** The LHC results on the sub-leading flow modes in PbPb collisions at 2.76 TeV, related to initial-state fluctuations, are analyzed and interpreted within the HYDJET++ model. Using the newly introduced Principal Component Analysis (PCA) method applied to two-particle azimuthal correlations extracted from the model calculations, the leading and the sub-leading flow modes are studied as a function of the transverse momentum ( $p_T$ ) over a wide centrality range. The leading modes of the elliptic ( $v_2^{(1)}$ ) and triangular ( $v_3^{(1)}$ ) flow calculated within the HYDJET++ model reproduce rather well the  $v_2\{2\}$  and  $v_3\{2\}$  coefficients experimentally measured using the two-particle correlations. Within the  $p_T \leq 3$  GeV/c range where hydrodynamics dominates, the sub-leading flow effects are greatest at the highest  $p_T$  of around 3 GeV/c. The sub-leading elliptic flow mode ( $v_2^{(2)}$ ), which corresponds to  $n = 2$  harmonic, has a small non-zero value and slowly increases from central to peripheral collisions, while the sub-leading triangular flow mode ( $v_3^{(2)}$ ), which corresponds to  $n = 3$  harmonic, is even smaller and does not depend on centrality. For  $n = 2$ , the relative magnitude of the effect measured with respect to the leading flow mode shows a shallow minimum for semi-central collisions and increases for very central and for peripheral collisions. For  $n = 3$  case, there is no centrality dependence. The sub-leading flow mode results obtained from the HYDJET++ model are in a rather good agreement with the experimental measurements of the CMS Collaboration.

### 1 Introduction

At sufficiently high energy density achieved in ultra-relativistic heavy-ion collisions, a new state of matter, called Quark-Gluon-Plasma (QGP), is created. The QGP is characterized by collective expansion described by relativistic hydrodynamics. Due to the different pressure gradients in different directions, the initial spatial eccentricity converts into momentum anisotropy. Quantitatively, the anisotropy is described by Fourier decomposition of the azimuthal angle ( $\phi$ ) hadron distribution [1–3]

$$\frac{dN}{d\phi} \propto 1 + 2 \sum_n v_n \cos[n(\phi - \Psi_n)], \quad (1)$$

where Fourier coefficients,  $v_n$ , characterize magnitude of the azimuthal anisotropy measured with respect to the flow symmetry plane angle,  $\Psi_n$  [4]. The angle  $\Psi_n$  determines the direction of maximum

<sup>a</sup>e-mail: Jovan.Milosevic@cern.ch

final-state particle density. The second order Fourier coefficient,  $v_2$ , is called elliptic flow. The angle  $\Psi_2$  corresponds to the flow symmetry plane spanned over the beam direction and the shorter axis of the roughly elliptical shape of the nucleon overlap region. Due to the initial-state fluctuations of the position of nucleons at the moment of impact, higher-order deformations of the initial geometry are induced leading to the appearance of higher-order Fourier harmonics ( $v_n, n \geq 3$ ). The collective behavior of the QGP has been studied using the azimuthal anisotropy of particles detected at experiments at the Relativistic Heavy Ion Collider (RHIC) [5–7]. The studies have been continued also with the experiments [8–19] at the Large Hadron Collider (LHC) at significantly higher collision energies.

Another experimental method to determine the  $v_n$  coefficients uses two-particle azimuthal correlations [20] which can be also Fourier decomposed as

$$\frac{dN^{pair}}{d\Delta\phi} \propto 1 + 2 \sum_n V_{n\Delta} \cos(n\Delta\phi), \quad (2)$$

where  $\Delta\phi$  is a relative azimuthal angle of a particle pair. The two-particle Fourier coefficient  $V_{n\Delta}$  is expected to factorize as

$$V_{n\Delta}(p_T^a, p_T^b) = v_n(p_T^a)v_n(p_T^b), \quad (3)$$

into a product of the anisotropy harmonics  $v_n$ .

The Eq. (3) is correct if the angle  $\Psi_n$  in Eq. (1) is a global quantity for a given collision. The factorization breaking effect has been theoretically predicted in [21, 22]. It is shown that even if the hydrodynamic flow is the only source of the two-particle correlations, initial-state fluctuations turn the  $\Psi_n$  from a global to both,  $p_T$  and pseudorapidity<sup>1</sup> ( $\eta$ ) dependent quantity. Lumpy hot-spots raised from the initial-state fluctuations can generate a local pressure gradient which makes the corresponding local flow symmetry plane to be slightly different but still correlated with the global  $\Psi_n$ . This effect of initial-state fluctuations thus breaks the factorization relation of Eq. (3). A significant breakdown of the factorization assumption has been observed both in the transversal  $p_T$  and longitudinal  $\eta$  direction in symmetric PbPb collisions [18, 19, 23] as well as in asymmetric pPb collisions [19, 23].

A new approach which employs the Principal Component Analysis (PCA) to study the flow phenomena is introduced in [24, 25]. Using a PCA approach,  $V_{n\Delta}$  coefficients as a function of both particles  $p_T$  are represented through the leading and the sub-leading flow mode terms. The leading flow modes are essentially equivalent to anisotropy harmonics  $v_n\{2\}$  extracted from two-particle correlations. As a consequence of initial-state fluctuations, the sub-leading flow modes appear as the largest sources of factorization breaking. The PCA study of this effect gives new insights into the expansion dynamics of the QGP, and serves as an excellent tool for testing the hydrodynamical models.

## 2 HYDJET++

The Monte Carlo HYDJET++ model [26] simulates relativistic heavy ion collisions in an event-by-event manner. It consists of two components which simulate soft and hard processes. The soft part provides the hydrodynamical evolution of the system while the hard part describes multiparton fragmentation within the formed medium. Within the hard part, jet quenching effects are taken into account. The hard part of the model consists of PYTHIA [27] and PYQUEN [28] event generators. Within the soft part, the magnitude of the flow is regulated by spatial anisotropy  $\epsilon(b)$  at a given impact parameter vector<sup>2</sup> magnitude  $b$ , and by momentum anisotropy  $\delta(b)$ . The events can be generated under several switches. The most realistic one, 'flow+quenched jets', includes both hydrodynamics expansion and quenched jets. In this analysis, the pure 'flow' switch is also used.

<sup>1</sup>Pseudorapidity  $\eta$  is defined as  $-\ln \tan(\theta/2)$  where  $\theta$  is the polar angle.

<sup>2</sup>In an ideal circle-like geometry, impact parameter  $\vec{b}$  is a vector which connects centers of the colliding nuclei.

### 3 Two-particle correlation function

The definition of the two-dimensional (2D) two-particle correlation function is adopted from the CMS experiment. Any charged pion from the  $|\eta| < 2$  range is used as a 'trigger' particle. In order to perform a differential analysis, events are divided into eight centrality classes<sup>3</sup>, while the analyzed  $p_T$  range has seven non-equidistant intervals. Since in an event there can be more than one trigger particle from a given  $p_T$  interval, the corresponding total number is denoted by  $N_{trig}$ . In each event, trigger particle is paired with all charged pions from the  $|\eta| < 2$  range within a given  $p_T$  interval. The signal distribution,  $S(\Delta\eta, \Delta\phi)$ , is defined as the yield of the per-trigger-particle pairs,  $N^{same}$ ,

$$S(\Delta\eta, \Delta\phi) = \frac{1}{N_{trig}} \frac{d^2 N^{same}}{d\Delta\eta d\Delta\phi}, \quad (4)$$

in a given  $(\Delta\eta, \Delta\phi)$  bin where  $\Delta\eta$  and  $\Delta\phi$  are corresponding differences in  $\eta$  and  $\phi$  between the two charged pions which form the pair. The background distribution,  $B(\Delta\eta, \Delta\phi)$ , is constructed using the technique of mixing topologically similar (relative difference in multiplicity smaller than 5%) events. The trigger particles from one event are mixed with the associated particles from a different event. To reduce contribution to the statistical uncertainty from the background distribution, associated particles from 10 randomly chosen events are used. In the background distribution, defined as

$$B(\Delta\eta, \Delta\phi) = \frac{1}{N_{trig}} \frac{d^2 N^{mix}}{d\Delta\eta d\Delta\phi}, \quad (5)$$

$N^{mix}$  denotes the number of mixed-event pairs in a given  $(\Delta\eta, \Delta\phi)$  bin. As the  $B(\Delta\eta, \Delta\phi)$  is formed from uncorrelated particles, it gives a distribution of independent particle emission.

The 2D two-particle differential correlation function is then defined as the normalized ratio<sup>4</sup>

$$\frac{1}{N_{trig}} \frac{d^2 N^{pair}}{d\Delta\eta d\Delta\phi} = B(0, 0) \frac{S(\Delta\eta, \Delta\phi)}{B(\Delta\eta, \Delta\phi)}. \quad (6)$$

In order to obtain  $v_n\{2\}$  harmonics, the projection of the 2D correlation function given by Eq. (6) onto  $\Delta\phi$  axis can be Fourier decomposed as given in Eq. (2). In order to suppress the short-range correlations arising from jet fragmentation and resonance decays, an averaging over  $|\Delta\eta| > 2$  is applied.

### 4 Principle Component Analysis

PCA is a method that orders fluctuations in data by so-called components. Application of the PCA in frames of anisotropic flow was introduced in [24, 25, 29]. By extracting principal components from the two-particle correlation data one can probe the presence of initial-state fluctuations. An approach for calculating the  $V_{n\Delta}$  harmonics, alternative to the one shown in Section 3, is applied in [18] as,

$$V_{n\Delta}(p_T^a, p_T^b) = \langle\langle \cos(n\Delta\phi) \rangle\rangle_S - \langle\langle \cos(n\Delta\phi) \rangle\rangle_B. \quad (7)$$

Here, double brackets  $\langle\langle \cdot \rangle\rangle$  denote averaging over charged pion pairs and over all events from the given centrality class. The procedure of forming pairs in  $S$  and  $B$ , with the pseudo-rapidity cut  $|\Delta\eta| > 2$ , is identical as in Section 3. Following the procedure given in [24], in order to use the PCA technique a single bracket definition for the two-particle Fourier harmonics  $V_{n\Delta}^{PCA}$  is used,

$$V_{n\Delta}^{PCA}(p_T^a, p_T^b) = \langle \cos(n\Delta\phi) \rangle_S - \langle \cos(n\Delta\phi) \rangle_B, \quad (8)$$

<sup>3</sup>The centrality is defined as a fraction of the total inelastic PbPb cross section, with 0% denoting the most central collisions.

<sup>4</sup>The normalization factor,  $B(0, 0)$ , is the value of the background distribution at  $\Delta\eta = 0$  and  $\Delta\phi = 0$ .

where  $\langle \cdot \rangle$  refers to averaging over all events from the given centrality class. The PCA method is applied by doing the eigenvalue decomposition of the covariance matrix that is built out of the  $V_{n\Delta}^{PCA}$  harmonics. By defining  $N_b$  differential  $p_T$  bins one can construct the corresponding covariance matrix  $[\hat{V}(p_T^a, p_T^b)]_{N_b \times N_b}$ . The diagonal elements are harmonics with correlated particles  $a$  and  $b$  taken from the same  $p_T$  bin and the non-diagonal elements are harmonics with correlated particles  $a$  and  $b$  taken from the different  $p_T$  bins. By solving the eigenvalue problem of the  $[\hat{V}(p_T^a, p_T^b)]_{N_b \times N_b}$  matrix, a set of the eigenvalues,  $\lambda^{(\alpha)}$ , and eigenvectors,  $e^{(\alpha)}$ , has been obtained. Here,  $\alpha = 1, \dots, N_b$ . A new  $p_T$ -dependent observable,  $V_n^{(\alpha)}(p_T)$ , is introduced as

$$V_n^{(\alpha)}(p_T) = \sqrt{\lambda^{(\alpha)}} e^{(\alpha)}(p_T), \quad (9)$$

referring to it as mode for the given  $\alpha$ . The first mode ( $\alpha = 1$ ) corresponds to the first greatest variance of data, the second mode ( $\alpha = 2$ ) corresponds to the second greatest variance of data and so on. A normalized mode is defined as,

$$v_n^{(\alpha)}(p_T) = \frac{V_n^{(\alpha)}(p_T)}{\langle M(p_T) \rangle}, \quad (10)$$

where  $\langle M(p_T) \rangle$  denotes the averaged multiplicity in a given  $p_T$  bin. The procedure is described in details in [30]. The observables from Eq. (10) for  $\alpha = 1$  and  $\alpha = 2$  will be referred to as the leading and the sub-leading flow modes respectively. The magnitude of the leading flow mode,  $v_n^{(1)}$ , should be practically equal to the  $v_n\{2\}$  measured using the two-particle correlation method. The CMS Collaboration showed in [30, 31] that the  $p_T$  dependence of the leading elliptic and triangular flow modes for pPb collisions at 5.02 TeV and for PbPb collisions at 2.76 TeV data are in excellent agreement with corresponding two-particle measurements presented in [32] and in [33], respectively.

## 5 Results

In order to check the consistency of extracted  $v_n$  harmonics using the method of PCA and one of the standard approaches given by Eq. (2), as well as to perform a PCA analysis in order to extract the leading and sub-leading flow modes, the two-particle correlation functions defined by the Eq. (6) are constructed. For each centrality interval, ranged from the ultra-central 0-0.2% till peripheral 50-60%, two-particle correlation functions for 7  $p_T$  intervals between 0.3 and 3.0 GeV/c are formed.

In Fig. 1 are shown the PCA results on the leading and sub-leading flow modes for the second harmonic in 8 centrality regions ranged for PbPb collisions at  $\sqrt{s_{NN}} = 2.76$  TeV simulated within HYDJET++ event generator. The leading flow mode,  $v_2^{(1)}$ , is dominant and rather well describes the experimentally measured  $v_2\{2\}$  from two-particle correlations taken from [18] and [33]. Additionally, due to consistency, in Fig. 1 are also shown  $v_2\{2, |\Delta\eta| > 2\}$  values measured using two-particle correlations constructed from the same HYDJET++ generated data. In Fig. 1 these results are depicted with crosses and show an excellent agreement with  $v_2^{(1)}$  extracted using the PCA method. The extracted  $v_2^{(1)}$  has expected centrality behavior: a small magnitude at ultra-central collisions which then gradually increases going to peripheral collisions. The newly observed sub-leading flow mode of second order harmonic,  $v_2^{(2)}$ , is practically equal to zero at small- $p_T$  for all centrality bins. For  $p_T > 2$  GeV/c, the sub-leading flow mode has a small positive value and slowly increases going from semi-central to peripheral PbPb collisions. The CMS collaboration presented in [30, 31] experimentally measured the leading and sub-leading flow mode in PbPb collisions within the same  $p_T$  range and for the same centrality bins as it is adopted in this analysis. Beside the leading flow mode, HYDJET++ predictions for the sub-leading flow mode are also in a qualitative agreement with the experimental results from [30, 31]. For centralities above 30%, the  $v_2^{(2)}$  magnitudes predicted by HYDJET++ model are slightly larger with respect to the ones observed from the experimental data.

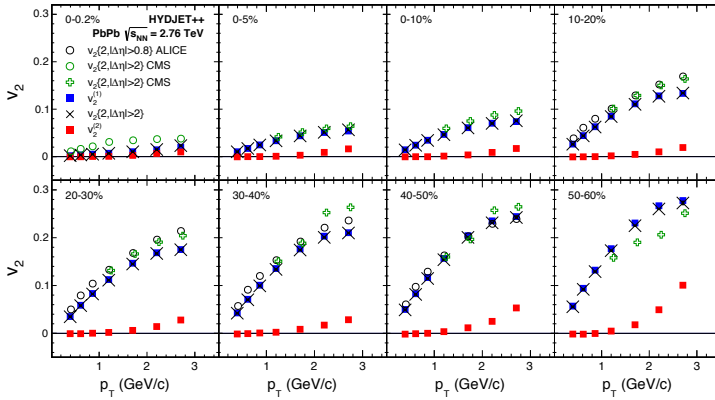


**Figure 1.** The leading ( $\alpha = 1$ ) and the sub-leading ( $\alpha = 2$ ) flow mode for  $n = 2$  case as a function of  $p_T$  measured using the PCA in a wide centrality range of PbPb collisions at 2.76 TeV generated within the HYDJET++ model. The  $v_2^{(1)}$  results are compared to the  $v_2\{2\}$  measured by the CMS [18] (open green circles) and [15] (open green crosses) and by ALICE [33] collaborations, and to the  $v_2\{2, |\Delta\eta| > 2\}$  extracted from the same HYDJET++ simulation using the two-particle correlations. The error bars correspond to statistical uncertainties.

Similarly as in Fig. 1, in Fig. 2 are shown the PCA leading and sub-leading flow mode predictions of HYDJET++ model for the third harmonic. Again, the results are extracted from the 8 centrality regions, same as in Fig. 2, of PbPb collisions at  $\sqrt{s_{NN}} = 2.76$  TeV. The  $v_3^{(1)}$  is in a rather good agreement with the  $v_3\{2\}$  results measured using two-particle correlations taken from [18] and [33], except in the case of ultra-central collisions. Also, the  $v_3\{2\}$  extracted from the two-particle correlations formed from the same HYDJET++ generated data are in an excellent agreement with the  $v_3^{(1)}$  obtained from the PCA method. The sub-leading mode is, up to 3 GeV/c, almost equal to zero. This supports results from [19, 23] that the third harmonic factorizes better than the second one. Also, the small  $v_3^{(2)}$  values extracted from HYDJET++ simulated PbPb events are in an agreement with those found in [30, 31] extracted from the experimental PbPb data.

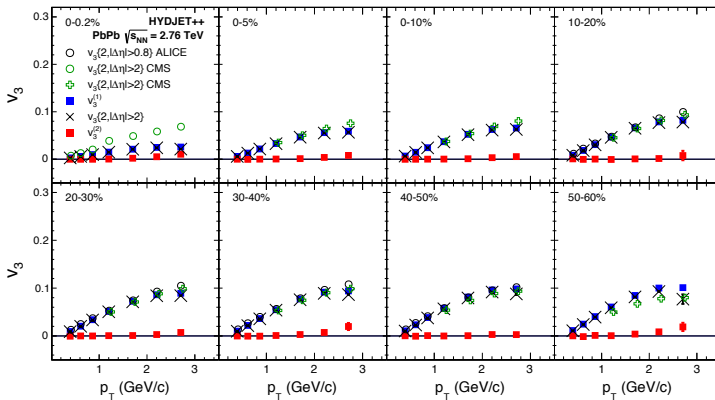


**Figure 2.** The leading ( $\alpha = 1$ ) and the sub-leading ( $\alpha = 2$ ) flow mode for  $n = 3$  case as a function of  $p_T$  measured using the PCA in a wide centrality range of PbPb collisions at 2.76 TeV generated within the HYDJET++ model. The  $v_3^{(1)}$  results are compared to the  $v_3\{2\}$  measured by the CMS [18] (open green circles) and [15] (open green crosses) and by the ALICE [33] collaborations, and to the  $v_3\{2, |\Delta\eta| > 2\}$  extracted from the same HYDJET++ simulation using the two-particle correlations. The error bars correspond to statistical uncertainties.

In order to summarize results, in Fig. 3 are depicted ratios between the sub-leading and leading flow mode. The ratio is calculated from the values taken from  $2.5 < p_T < 3.0$  GeV/c where the

effect is strongest. The results are presented as a function of centrality. The results in the top panel of Fig. 3 show that in the case of  $n = 2$  the strength of the relative magnitude  $v_2^{(2)}/v_2^{(1)}$  is smallest for events with centralities between 10 and 30%, i.e. where the elliptic flow is most pronounced. Going to very central collisions, the magnitude of the effect dramatically increases. Also, the effect reaches a significant magnitude going to peripheral collisions. Qualitatively, such behavior is in an agreement with the  $r_2$  multiplicity dependence presented in [19]. Centrality dependence of the ratio which corresponds to the  $n = 3$  case is shown in the bottom panel of Fig. 3. The  $v_3^{(2)}/v_3^{(1)}$  ratio, integrated over all centralities, is  $0.095 \pm 0.009$ . The overall small  $v_3^{(2)}$  values found in this analysis are also in a qualitative agreement with the  $r_3$  multiplicity dependence presented in [19].

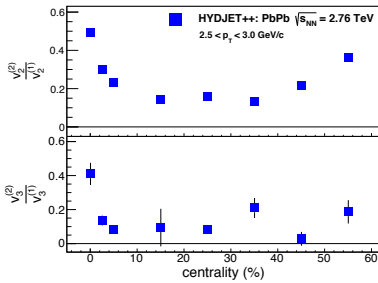


**Figure 3.** The ratio between values of the sub-leading and leading flow, taken for the highest  $p_T$  bin, as a function of centrality calculated using the PCA method applied to PbPb collisions at  $\sqrt{s_{NN}} = 2.76$  TeV simulated with the HYD- JET++ event generator. The error bars correspond to statistical uncertainties.

## 6 Discussion

In order to explore the origin of the sub-leading flow observed in the HYDJET++ model, beside the PbPb data analysis obtained under the 'flow + quenched jets' switch which results are shown in Sect. 5, the pure 'flow' switch has been used to generate PbPb collisions at  $\sqrt{s_{NN}} = 2.76$  TeV too. The comparisons between the PCA  $v_2$  and  $v_3$  results obtained under these two switches are shown in Fig. 4 and Fig. 5, respectively. As expected, the pure 'flow' HYDJET++ switch gives a linearly increasing leading flow mode for both  $v_n^{(1)}$  harmonics  $n = 2$  and 3. Also, as expected, the corresponding magnitude, at a given  $p_T$ , is greater with respect to the one extracted from the data obtained under 'flow + quenched jets' switch. The results for the sub-leading flow mode obtained under pure 'flow' switch, contrary to those shown in Sect. 5 are consistent with zero for centralities smaller than 20%. But, even in the case of the pure 'flow' switch, for centralities above 20% a modest effect of the sub-leading flow starts to appear. Up to the centrality of 40% the magnitude of the effect is still smaller with respect to the both, experimental results from [30, 31] and from the results obtained using the 'flow + quenched jets' switch. For the most peripheral, 50-60% the  $v_2^{(2)}$  magnitude at high enough  $p_T$  is greater than the experimental one and the one obtained under the 'flow + quenched jets' switch.

At first glance, it seems that HYDJET++ data simulated under the pure 'flow' switch should not show existence of the sub-leading flow modes. But, resonance decays and fluctuations of particle momenta together with the topology of peripheral events [34] could imitate hot-spots which at the end could produce a non-zero sub-leading flows. The HYDJET++ data simulated under the 'flow + quenched jets' could have charged pions coming from the jet fragmentation, which due to the interaction with the soft medium and because of different path length with respect to the flow symmetry plane can increase abundance of such high- $p_T$  pions near the flow symmetry plane. This also could produce the above mentioned hot-spots and consequently sub-leading flows.

The results for the sub-leading triangular flow mode are presented in Fig. 4. Similarly to the 'flow + quenched jets' results shown in Sect. 5, the  $v_3^{(2)}$  values, calculated using the pure 'flow' switch, are

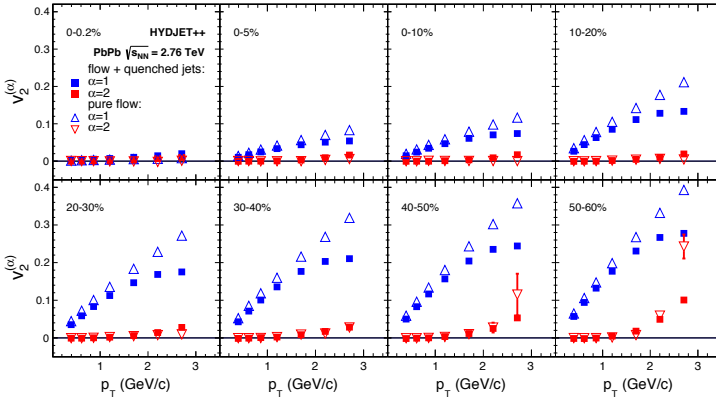


**Figure 4.** The leading ( $\alpha = 1$ ) and the sub-leading ( $\alpha = 2$ ) flow mode for  $n = 2$  case as a function of  $p_T$  measured using the PCA in a wide centrality range of PbPb collisions at 2.76 TeV generated within the HYDJET++ model under the pure 'flow' switch (triangles) and under the 'flow + quenched jets' switch (squares). The error bars correspond to statistical uncertainties.

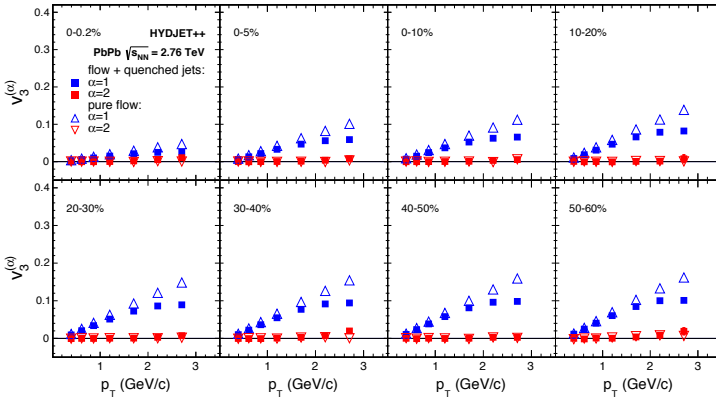


**Figure 5.** The leading ( $\alpha = 1$ ) and the sub-leading ( $\alpha = 2$ ) flow mode for  $n = 3$  case as a function of  $p_T$  measured using the PCA in a wide centrality range of PbPb collisions at 2.76 TeV generated within the HYDJET++ model under the pure 'flow' switch (triangles) and under the 'flow + quenched jets' switch (squares). The error bars correspond to statistical uncertainties.

close to zero for all centralities and at all  $p_T$ . This again shows that the assumption of the factorization of the two-particle Fourier coefficients into a product of the  $v_3$  anisotropy harmonics in the case of the pure 'flow' switch is fully valid.

The Pearson coefficient, used to measure the magnitude of the effect is defined [19, 24] as

$$r_n(p_T^a, p_T^b) = \frac{V_{n\Delta}(p_T^a, p_T^b)}{\sqrt{V_{n\Delta}(p_T^a, p_T^a)V_{n\Delta}(p_T^b, p_T^b)}} \sim \langle \cos n(\Psi_n(p_T^a) - \Psi_n(p_T^b)) \rangle. \quad (11)$$

The  $r_n$  ratio is equal to one if the flow symmetry plane angle is a global quantity. If the factorization breaking occurs then the value of the  $r_n$  becomes smaller than one. In [24] it is shown that the principal component analysis approximates the two-particle Fourier coefficient as

$$V_{n\Delta}(p_T^a, p_T^b) = \sum_{\alpha=1}^{N_b} V_n^{(\alpha)}(p_T^a) V_n^{(\alpha)*}(p_T^b), \quad (12)$$



where each term in the sum corresponds to a different mode  $\alpha$  of the flow fluctuations introduced with Eq. (9). Factorization breaking occurs when non-zero terms with  $\alpha \geq 2$  appears in the above sum. Eq. (12) is used to reconstruct  $V_{n\Delta}$  coefficients from  $V_n^{(\alpha)}$  flow modes extracted within the principal component analysis. In order to connect the results on the sub-leading flow modes extracted from HYDJET++ generated PbPb collisions at 2.76 TeV with the experimentally seen initial-state fluctuations [19], in Fig. 6 is shown comparison between the  $r_2$  and  $r_3$  ratios, depicted as a function of the transverse momentum difference  $p_T^a - p_T^b$ , measured experimentally in [19] and those extracted from HYDJET++ model and calculated using Eq. (11) and Eq. (12). The comparison is performed only in ultra-central (0-0.2% centrality) and peripheral (40-50% centrality) collisions, i.e. where the factorization effect is largest. Using in Eq. (12) only the leading and sub-leading flow mode ( $N_b = 2$ ) one observes a fair reconstruction of  $r_n$  ratios. To improve the reconstruction of  $r_2$  in ultra-central collisions where the effect of the initial-state fluctuations dominates, one would need to add additional modes ( $\alpha \geq 3$ ) in the two-particle harmonic decomposition. As in the case of the elliptic flow, the sub-leading flow mode corresponding to the triangular flow captures the small factorization effect well.

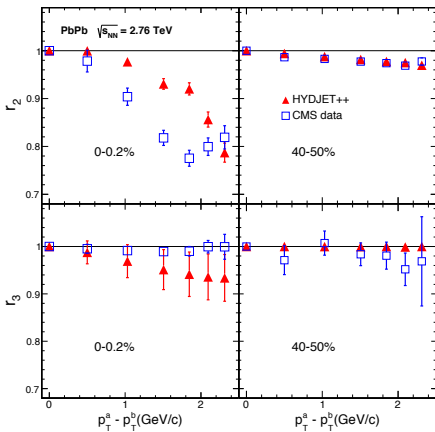


**Figure 6.** Comparison of  $r_2$  (top row) and  $r_3$  (bottom row) reconstructed with harmonic decomposition using the leading and sub-leading flow mode extracted from HYDJET++ model with the experimental  $r_2$  and  $r_3$  values taken from [19] for the ultra-central 0-0.2% and peripheral 40-50% centrality classes in PbPb collisions at  $\sqrt{s_{NN}} = 2.76$  TeV. The error bars correspond to statistical uncertainties.

## 7 Conclusions

The PCA method for studying flow, by its construction, may fully exploits the information contained in the covariance matrix formed from the two-particle Fourier coefficients and thus may provide high sensitivity not only to the standardly defined flow measurements, but also to the influence of the initial-state fluctuations to the hydrodynamic flow. In difference of two-particle correlation method where the information was calculated by integrating over momentum of one of particles which form the pair, within the PCA approach, the detailed information depends on the momenta of both particles of the pair. As the leading flow mode represents the hydrodynamic response to the average geometry, it is essentially equal to the anisotropy harmonics measured using the two-particle correlations method. The sub-leading mode could be understood as the response to the event-by-event initial-state fluctuations which are the main source of the factorization-breaking effect.

The PCA analysis of the PbPb collisions simulated by HYDJET++ model at  $\sqrt{s_{NN}} = 2.76$  GeV shows that the leading flow mode,  $v_n^{(1)}$ , for  $n = 2, 3$  represents dominant mode and qualitatively describes the experimentally measured  $v_n$  from two-particle correlations. Additionally, HYDJET++



model also shows existence of the sub-leading flow mode  $v_n^{(2)}$  which magnitude is in a rather good agreement with the experimental results from the CMS Collaboration. Also, the  $r_2$  and  $r_3$  ratios calculated from only leading and sub-leading flow modes extracted from HYDJET++ model data using the PCA fairly reconstructs experimentally measured ratios. This analysis may also provide new insights into the possible influence of the dynamics of the collision onto appearance of the sub-leading flow modes, and help to understand and improve modeling of the QGP evolution.

## References

- [1] J.-Y. Ollitrault, Phys. Rev. D **48** 1132 (1993)
- [2] S. Voloshin and Y. Zhang, Z. Phys. C **70** 665 (1996)
- [3] A. M. Poskanzer and S. A. Voloshin, Phys. Rev. C **58** 1671 (1998)
- [4] B. Alver and G. Roland, Phys. Rev. C **81** 054905 (2010)
- [5] B.B. Back et al. (PHOBOS Collaboration), Phys. Rev. Lett., **89** 222301 (2002)
- [6] K.H. Adams et al. (STAR Collaboration), Phys. Rev. Lett., **86** 402 (2001)
- [7] K. Adcox et al. (PHENIX Collaboration), Phys. Rev. Lett. **89** 212301 (2002)
- [8] K. Aamodt et al. (ALICE Collaboration), Phys. Rev. Lett. **105** 252302 (2010)
- [9] K. Aamodt et al. (ALICE Collaboration), Phys. Rev. Lett. **107** 032301 (2011)
- [10] B.B. Abelev et al. (ALICE Collaboration), JHEP **1506** 190 (2015)
- [11] J. Adam et al. (ALICE Collaboration), Phys. Rev. Lett. **116** 132302 (2016)
- [12] G. Aad et al. (ATLAS Collaboration), Phys. Lett. B **707** 330 (2012)
- [13] G. Aad et al. (ATLAS Collaboration), Phys. Rev. C **86** 014907 (2012)
- [14] G. Aad et al. (ATLAS Collaboration), JHEP **11** 183 (2013)
- [15] S. Chatrchyan et al. (CMS Collaboration), Eur. Phys. J. C **72** 2012 (2012)
- [16] S. Chatrchyan et al. (CMS Collaboration), Phys. Rev. C **87** 014902 (2013)
- [17] S. Chatrchyan et al. (CMS Collaboration), Phys. Rev. C **89** 044906 (2014)
- [18] S. Chatrchyan et al. (CMS Collaboration), JHEP **02** 088 (2014)
- [19] V. Khachatryan et al. (CMS Collaboration), Phys. Rev. C **92** 034911 (2015)
- [20] S. Wang et al., Phys. Rev. C **44** 1091 (1991)
- [21] F. G. Gardim, F. Grassi, M. Luzum, and J.-Y. Ollitrault, Phys. Rev. C **87** 031901 (2013)
- [22] U. Heinz, Z. Qiu, and C. Shen, Phys. Rev. C **87** 034913 (2013)
- [23] Y. Zhou, Nucl. Phys. A **931** 949 (2014)
- [24] R. Bhalerao, J.-I. Ollitrault, S. Pal, and D. Teaney, Phys. Rev. Lett. **114** 152301 (2015)
- [25] A. Mazeliauskas and D. Teaney, Phys. Rev. C **91** 044902 (2015)
- [26] I.P. Lokhtin, L.V. Malinina, S.V. Petrushanko, A.M. Snigirev, I. Arsene, and K. Tywoniuk, Comput. Phys. Commun. **180** 779 (2009)
- [27] T. Sjostrand, S. Mrenna, and P. Skands, JHEP **0605** 026 (2006)
- [28] I.P. Lokhtin and A.M. Snigirev, Eur. Phys. J. C **45** 211 (2006)
- [29] A. Mazeliauskas and D. Teaney, Phys. Rev. C **93** 024913 (2016)
- [30] CMS Collaboration, CMS-HIN-15-010, (2015), <http://cds.cern.ch/record/2055291>
- [31] J. Milosevic for the CMS Collaboration, Nucl. Phys. A **956** 308 (2016)
- [32] S. Chatrchyan et al. (CMS Collaboration), Phys. Lett. B **724** 213 (2013)
- [33] K. Aamodt et al. (ALICE Collaboration), Phys. Lett. B **708** 249 (2012)
- [34] L. V. Bravina, E. S. Fotina, V. L. Korotkikh, I. P. Lokhtin, L. V. Malinina, E. N. Nazarova, S. V. Petrushanko, A. M. Snigirev, E. E. Zabrodin, Eur. Phys. J. C **75** 588 (2015)